Chapter 3

HUMAN RANVIER NODE MODEL

Smit, J. E., Hanekom, T. and Hanekom, J. J. (2008) Modelled temperature-dependent excitability behaviour of a single Ranvier node for a human peripheral sensory nerve fibre, *in review*

3.1 INTRODUCTION

The present study focusses on the development of a new human Type I ANF model. The ANF model is developed in three phases. This chapter deals with the first phase, namely the development of the human Ranvier node model. Its objective is to determine whether the Hodgkin-Huxley (HH) model for unmyelinated nerve fibres can be modified to describe action potential dynamics at Ranvier nodes using recorded ionic membrane current data from single human myelinated peripheral nerve fibres (Reid *et al.*, 1993; Scholz *et al.*, 1993; Schwarz *et al.*, 1995; Reid *et al.*, 1999) together with the temperature dependency of all parameters. Only the model parameters are modified to those of human, with the equations left unaltered. This model is developed as part of a larger model to describe excitation behaviour in a generalised human peripheral sensory nerve fibre.

3.2 MODEL AND METHODS

3.2.1 Parameters applied to the nodal model

In the original Hodgkin-Huxley (Hodgkin and Huxley, 1952) formulation, the change in the membrane potential (V) is described by

$$C_m \frac{dV}{dt} = -I_{ion} + I_{stim} \qquad \left[\mu A/cm^2\right], \tag{3.1}$$

with V offset by the resting membrane potential (V_{res}) and having an initial value $V(0)$ equal to 0. The time dependent ionic membrane current (I_{ion}) consists of a fast activating and inactivating sodium ion (I_{Na}) current, a fast activating potassium ion (I_{Kf}) current and a leakage (I_L) current

$$I_{ion} = g_{Na}^{max} m^3 h \left(V - V_{Na}\right) + g_K^{max} n^4 \left(V - V_K\right) + g_L \left(V - V_L\right) \qquad \left[\mu A/cm^2\right]. \tag{3.2}$$

Ionic currents are considered ohmic and are given in terms of the ionic conductances and change in membrane potential. Ion channel activation and inactivation probability dynamics (m, h and n respectively) are described by

$$\frac{dx}{dt} = \alpha_x \left(V\right)\left[1 - x\right] - \beta_x \left(V\right) x, \quad x = m, n, h \tag{3.3}$$

with initial values $m(0) = 0.5$, $h(0) = 0.6$, $n(0) = 0.32$, and given in terms of the voltage dependent opening and closing rates of the ion channels $\alpha(V)$ and $\beta(V)$; the latter giving an indication of the membrane's permeability to the specific species of ion.

In this study, the above equation set was modified by changing the parameter values describing the ionic and leakage conductances, corresponding equilibrium potentials, the membrane rest potential and membrane capacitance to reflect the corresponding parameter values of human, while leaving the equations unaltered. These parameters are considered temperature independent in the original HH model and only the temperature dependence of the ion channel activation and inactivation rate equations is taken into account through the use of Q_{10} factors (Hodgkin and Huxley, 1952). However, given the role that temperature plays in nerve fibre excitation behaviour, temperature dependency of the parameters was included into the new nodal model.

Lastly, the membrane's permeability to different ion species was increased or decreased by multiplying the $\alpha(V)$ and $\beta(V)$ rate equations by selected factors, as mentioned by Huxley in an article on the movement of ions during nerve stimulation (Huxley, 1959).

The ionic membrane currents in the new nodal model have been described in terms of temperature dependent sodium (g_{Na}), potassium (g_K) and leakage (g_L) ionic conductances, as well as ionic equilibrium potentials

$$\begin{aligned} I_{ion}(T) = g_{Na}^{max}(T)\, m^3 h\,(V - V_{Na}(T)) + g_K^{max}(T)\, n^4\,(V - V_K(T)) \\ + g_L(T)\,(V - V_L(T)) \qquad \left[\mu A/cm^2\right], \end{aligned} \tag{3.4}$$

and the $\alpha(V)$ and $\beta(V)$ rate equations by

$$\alpha_m, \alpha_{ns} = AQ_{10}^{(T-T_0)/10} \cdot \frac{B - CV}{D\,(\exp(B - CV)) - 1} \qquad [m/s], \tag{3.5a}$$

$$\beta_m, \beta_{ns}, \alpha_h = AQ_{10}^{(T-T_0)/10} \cdot B \exp\left(\frac{-V}{C}\right) \qquad [m/s], \tag{3.5b}$$

$$\beta_h = AQ_{10}^{(T-T_0)/10} \cdot \frac{1}{(1 + \exp(B - CV))} \qquad [m/s]. \tag{3.5c}$$

Acceleration of the activation and inactivation of the membrane's permeability to specific ion species, as suggested by Huxley (1959), is given by parameter **A** values (Table 3.1). Parameters **B**, **C** and **D** are the original HH model parameters which are considered constant (Hodgkin and Huxley, 1952).

In myelinated nerve fibres the total nodal I_{Na} is subdivided into two functionally distinct currents, where the largest proportion ($\sim 98\%$) has fast activating and inactivating kinetics (Burke *et al.*, 1999). Even though the HH model has a fast activating and inactivating I_{Na}, when an action potential simulated at 25 °C was compared to a similar human nerve fibre action potential from the Schwarz *et al.* (1995) study, the activation was too slow to describe the action potential rising phase in the human case. Activation and inactivation of I_{Na} was hence accelerated, as shown in Table 3.1 (parameter **A** values).

Voltage-gated potassium (K_v) channels provide a number of useful functions to the nerve fibre, including setting and regulating the membrane resting potential, regulating the amplitude and duration of action potentials and determining the frequency of firing (Hille, 2001). Three types of K_v channels have been measured in rat and human,

Table 3.1: Parameters used for calculation of the voltage dependent opening and closing rates of the ion channels.

Parameter	$\mathbf{Q_{10}}$	$\mathbf{T_0}$ **(°C)**	**A**	**B**	**C**	**D**
α_m	2.78	20	4.42	2.5	0.1	1
β_m	2.78	20	4.42	4.0	18	–
α_h	1.5	20	1.47	0.07	20	–
β_h	1.5	20	1.47	3.0	0.1	–
α_{ns}	1.5	20	0.20	1.0	0.1	10
β_{ns}	1.5	20	0.20	0.125	80	–

namely those with fast kinetics (K_f or F-channels), intermediate kinetics (K_i or I-channels) and slow kinetics (K_s or S-channels) (Röper and Schwarz, 1989; Reid *et al.*, 1993; Safronov *et al.*, 1993; Scholz *et al.*, 1993; Schwarz *et al.*, 1995). F- and I-channels cluster mostly under the myelin sheath, with only a few channels located at the node (Röper and Schwarz, 1989; Rasband, 2006). It has been suggested that these channels mediate I_{Kf}, but in mammals the activation of nodal I_{Kf} is too small to contribute significantly to the repolarisation of the action potential (Chiu *et al.*, 1979; Reid *et al.*, 1999). S-channels co-locate with sodium channels at the Ranvier node, where it activates and deactivates more slowly than the F- and I-channels and does not inactivate (Taylor, Burke and Heywood, 1992; Devaux, Kleopa, Cooper and Scherer, 2004; Schwarz, Glassmeier, Cooper, Kao, Nodera, Tabuena, Kaji and Bostock, 2006). Even though the S-channels' kinetics are considered too slow to contribute significantly to firing behaviour and are thus neglected in most models, a slow (I_{Ks}) potassium current is included in some human nerve fibre models (Schwarz *et al.*, 1995; Bostock and Rothwell, 1997). The HH model I_K contains only activation kinetics, which renders it suitable for use as I_{Ks}. Its activation kinetics was hence slowed down (parameter **A** values in Table 3.1).

Schwarz *et al.* (1995) measured ionic membrane currents and action potentials at Ranvier nodes from partially demyelinated human peripheral sensory nerve fibres, but no morphometric nerve fibre data were supplied. Wesselink *et al.* (1999) estimated the action potential rise and fall times and amplitudes at 20 and 25 °C from the aforementioned study, as well as predicted values at 37 °C, and these values were used for the nodal model validation.

Both Schwarz *et al.* (1995) and Wesselink *et al.* (1999) used a reference temperature

(T_0) of 20 °C, while Hodgkin and Huxley (1952) used a reference temperature (T_0) of 6.3 °C. To aid comparison with these models, the reference temperature for the new nodal model was changed to 20 °C. Optimisation of parameters was performed at this temperature and the action potential shape and amplitude compared to the corresponding estimated data from the aforementioned studies. Next, the temperature dependence of the rate equations, as expressed through Q_{10} factors, was determined by comparing simulated and estimated action potential shapes and amplitudes at 25 and 37 °C (Table 3.1).

Results from experimental studies by Reid *et al.* (1993), Scholz *et al.* (1993) and Schwarz *et al.* (1995) were used to deduce conductance and equilibrium potential values for the ionic membrane currents (Table 3.2). The equilibrium potentials were given in terms of the Nernst potential equations for the different ion species (Hille, 2001)

$$V_{Na}, V_K, V_L = \frac{1000RT_K}{F} \ln\left(\frac{[ion]_o}{[ion]_i}\right) - V_{rest} \qquad [mV]\,, \tag{3.6}$$

with R the universal gas constant, F the Faraday constant, T_K the absolute temperature (in Kelvin) and $[ion]_o/[ion]_i$ the extracellular to intracellular ion concentration ratio for Na^+, K^+ and leakage ions respectively (Table 3.2). The K^+ concentration ratio (K_{cr}) was calculated using the intra- and extracellular concentration values from Schwarz *et al.* (1995); who also measured a leakage current with a V_L of -84.0 mV at 20 °C, resulting in a leakage ion concentration ratio (L_{cr}) of about 0.036. This value was further optimised until the simulated action potential's recovery phase resembled those of the Schwarz study's action potential. Estimating a Na^+ concentration ratio (Na_{cr}) proved difficult, with previously reported values ranging from 4.4 to 14.05 (Scholz *et al.*, 1993; Schwarz *et al.*, 1995; Wesselink *et al.*, 1999; Hille, 2001). The value therefore had to be optimised for the model and this turned out to be only slightly higher than the original HH model value of 6.48 (Table 3.2).

Values for the resting membrane potential (V_{res}) at different temperatures were estimated by optimising the value until the membrane potential returned to 0 mV after stimulation. Hence, a value of -79.4 mV was estimated at 6.3 °C and became more negative as the temperature was increased to 37 °C, having a Q_{10} factor of 1.0356 for all $T \leq 20$ °C and 1.0345 for all $T > 20$ °C (Table 3.2). This gave a V_{rest} of -83.3 mV at 20 °C and -88.1 mV at 37 °C.

Table 3.2: Model electrical parameters.

Parameter	**Value**	**Q_{10}**	**T_0 (°C)**	**Reference**
Membrane resting potential (V_{rest})	-79.4 mV	1.0356 (T $\leq$ 20 °C) 1.0345 (T > 20 °C)	6.3	Hodgkin and Huxley (1952), Schwarz *et al.* (1995), Wesselink *et al.* (1999) †
Gas constant (R)	8.3145 J/K.mol			Atkins (1995)
Faraday constant (F)	9.6485×10^4 C/mol			Atkins (1995)
$[Na^+]_o/[Na^+]_i$	7.2102			Hodgkin and Huxley (1952), Schwarz *et al.* (1995), Wesselink *et al.* (1999), Hille (2001) #
$[K^+]_o/[K^+]_i$	0.0361			Reid *et al.* (1993), Scholz *et al.* (1993), Schwarz *et al.* (1995)
$[Leakage]_o/[Leakage]_i$	0.036645			Scholz *et al.* (1993), Schwarz *et al.* (1995) ††
Na^+ conductance (g_{Na})	640.00 mS/cm^2	1.1	24	Scholz *et al.* (1993), Hille (2001)
K^+ conductance (g_K)	60.0 mS/cm^2	1.16	20	Reid *et al.* (1993), Scholz *et al.* (1993), Schwarz *et al.* (1995) ††
Leakage conductance (g_L)	57.5 mS/cm^2	1.418	24	Schwarz and Eikhof (1987), Scholz *et al.* (1993), Schwarz *et al.* (1995) ††
Axoplasmic resistivity (ρ_{ax})	0.025 kΩ.cm	$(1.35)^{-1}$	37	Wesselink *et al.* (1999) †
Membrane capacitance (c_{mem})	2.8 μF/cm^2			Schwarz *et al.* (1995) *

† Value deduced from reference(s) and then optimised for model. Q_{10} value not from reference, but optimised for model

Discrepancy exists between HH model value and values for human. Value hence optimised for model

†† Values deduced from reference(s) and corrected for concentration and temperature differences

* Considered constant for temperatures between 20 °C and 42 °C

Since experimental study temperatures range from 20 – 27 °C, a Q_{10} factor for the potassium conductance (g_K) could be estimated. Leakage conductances (g_L) were measured by Scholz *et al.* (1993) and Schwarz *et al.* (1995), but not enough information was available to calculate the temperature dependence. However, g_L values were measured at 20 and 37 °C in rat, giving a Q_{10} factor of 1.418 (Schwarz and Eikhof, 1987). Estimation of the sodium conductance (g_{Na}) was more difficult, with only one study reporting a single channel value of about 13 pS (Scholz *et al.*, 1993). To convert the single channel conductance to a value for g_{Na}, the Na^+ channel density needed to be known and in mammals Na^+ channel densities vary between 700 and 2,000 /μm^2 (Hille, 2001). Also, the conductances of ion channels increase very little with a temperature increase, with Q_{10} factors typically in the vicinity of the values for aqueous diffusion; ranging from 1.0 – 1.6 in most cases (Hille, 2001). The values for g_{Na} and its Q_{10} factor played an important role in determining the action potential amplitude and were optimised by comparison with the calculated amplitudes at 20, 25 and 37 °C from Wesselink *et al.* (1999). To measure the time course and voltage dependence of activation and inactivation characteristics for ionic membrane currents, the current amplitude has to be sufficiently large so that it can be detected (Schwarz *et al.*, 2006). Hence, in experimental studies intra- and extracellular replacement Ringer solutions are substituted with isotonic concentration solutions to increase the current amplitudes, but this results in higher conductance values. Thus, conductance values had to be corrected for such concentration differences.

Similar to Wesselink *et al.* (1999) the electrical parameters were recalculated as values per unit area by assuming a fibre diameter of 15 μm and a nodal area of 50 μm^2. A nodal membrane capacitance (C_m) of 1.4 pF, i.e. a c_m of 2.8 μF.cm^{-2}, was used (Schwarz *et al.*, 1995). For squid, a positive temperature coefficient of about 1.36% per °C for C_m is found in the temperature range 3 – 21 °C, with no significant change in the range 21 – 42 °C and a sharp increase of at least 23% per °C for temperatures above 42 °C (Palti and Adelman Jr., 1969). Since no similar studies were performed for mammals, c_m was assumed to be constant over the temperature range 20 – 37 °C. The axoplasmic resistivity (ρ_{ax}) of the membrane did not influence the action potential shape and amplitude, and a value of 0.025 kΩ.cm at 37 °C and a Q_{10} factor of $(1.35)^{-1}$ were used (see Section 4.2).

3.2.2 Model output calculations

All the model output calculations were performed in Matlab. The modified equations were solved numerically using the ordinary differential equation (ODE) ode15s numerical solver, since they were too stiff to solve using the ode23t and ode45 solvers. The modelled node was externally stimulated using a monopolar external electrode positioned midway along the nodal length and 0.1 cm from the node. The external environment was considered infinite, isotropic and homogeneous with an external resistivity (ρ_e) of 0.3 kΩ.cm at 37 °C (Frijns *et al.*, 1994). External stimulation was thus considered purely resistive and given by

$$V_e = \frac{\rho_e I_{stim}}{4\pi r_{dist}} \quad [mV]\,, \tag{3.7}$$

with r_{dist} the distance between the node and the electrode.

Action potential (AP) characteristics include amplitude, duration, strength-duration behaviour, refractory period and conduction velocity. Since the nodal model only described APs generated at a single Ranvier node, refractory period and conduction velocity calculations could not be performed and have therefore not been dealt with in this chapter. AP duration is the sum of the rise and fall times. The AP is approximated by a triangle, with the apex at the maximum amplitude (Frijns and ten Kate, 1994). The rising edge intersects the AP curve at 10% of the maximum amplitude and the rise time is calculated as the time difference between this intersection point and the apex. The falling time is calculated in the same manner using the falling edge.

Rheobase current and chronaxie time characterises the strength-duration behaviour. Thresholds were calculated using a monopolar external electrode with monophasic-anodic stimulation pulses ranging from 0.2 – 2.0 ms in duration. The strength-duration curve was fitted with the linear relationship

$$I_{th}t = I_{rb}\,(t + \tau_{ch})\,, \tag{3.8}$$

with I_{th} the threshold current (μA), t the pulse duration (μs), I_{rb} the rheobase current (μA) and τ_{ch} the chronaxie time (μs) (Weiss, 1901; Bostock, 1983; Wesselink *et al.*, 1999).

The model's sensitivity to the different parameters was studied using sensitivity stud-

ies. At 25 °C, parameter values were varied from 20% to 100% of their optimised values, and their influence on the rise times, fall times and amplitudes were noted.

3.3 RESULTS

3.3.1 Action potential rise and fall times

A single Ranvier node from a general peripheral sensory nerve fibre was simulated in Matlab and externally stimulated with a monopolar electrode. Stimulation pulses were square, monophasic-anodic and only single pulses were used. The simulated node had a 15 μm diameter and 50 μm^2 area.

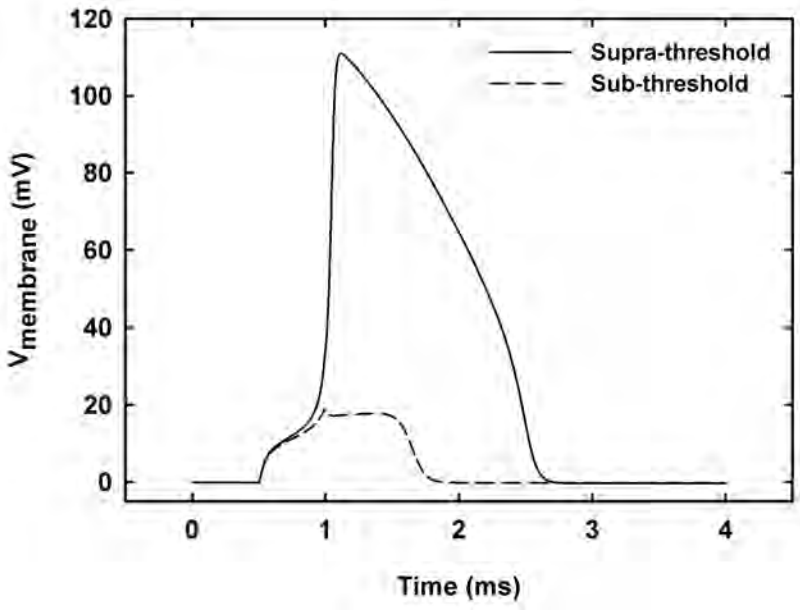

Figure 3.1: Sub-threshold and supra-threshold action potentials simulated at 25 °C.

APs were calculated at 20, 25 and 37 °C with rise and fall times compared to experimentally estimated results (Table 3.3). An example of sub-threshold and supra-threshold action potentials simulated at 25 °C are shown in Figure 3.1. The rise time

Table 3.3: Simulated characteristics of the human nodal model compared to experimentally estimated results from human Ranvier nodes.

Parameter	**Specifications**	**Value**		
	(15.0 μm fibre diameter)	**Human Node of Ranvier model**	**Experimental results**	**Reference**
Rise time (μs)	20 °C	270	270	Schwarz *et al.* (1995)
	25 °C	205	204	Schwarz *et al.* (1995)
	37 °C	123	120	Wesselink *et al.* (1999)
Fall time (μs)	20 °C	1870	1829	Schwarz *et al.* (1995)
	25 °C	1448	1464	Schwarz *et al.* (1995)
	37 °C	784	470	Wesselink *et al.* (1999)
Chronaxie (μs)	37 °C	65.5	64.9 $\pm$ 8.3	Bostock (1983)

was less than 0.5% longer than the estimated results at 25 °C and decreased by 24% (Q_{10} factor of $(1.73)^{-1}$) from 20 to 25 °C. The fall time was 2.2% longer at 20 °C and 1.1% shorter at 25 °C than the estimated results. Its decrease of 23% (Q_{10} factor of $(1.67)^{-1}$) was steeper than the 20% decrease (Q_{10} factor of $(1.56)^{-1}$) estimated from the experimental results.

Although no experimental data are available at 37 °C, a rise time of 120 μs and fall time of 470 μs has been estimated previously (Wesselink *et al.*, 1999). APs for the new nodal model had a 2.5% longer rise time and 67% longer fall time compared to these values.

Both rise and fall times were sensitive to sodium ion and leakage current parameters (Figures 3.2 and 3.3). Varying the sodium conductance Q_{10} factor values ($g_{Na}Q_{10}$) had a less than 7% influence on the rise and fall times. However, for Q_{10} values larger than 1.2 (i.e. relative parameter values larger than 1.03), the amplitude started to increase with an increase in temperature. This placed an upper limit on $g_{Na}Q_{10}$. Varying the sodium conductance (g_{Na}) had a more pronounced effect on the rise time than on the fall time. A decrease of 80% in g_{Na} increased the rise time by 100% and decreased the fall time by 70%. This was the same trend as observed for the sodium ion concentration ratio (Na_{cr}), with an increase of 30% in the rise time and a decrease of 20% in the fall time.

Surprisingly, varying the leakage current conductance (g_L) seemed to influence the rise and fall times as much as g_{Na} (Figures 3.2(b) and 3.3(b)). A 100% increase in g_L

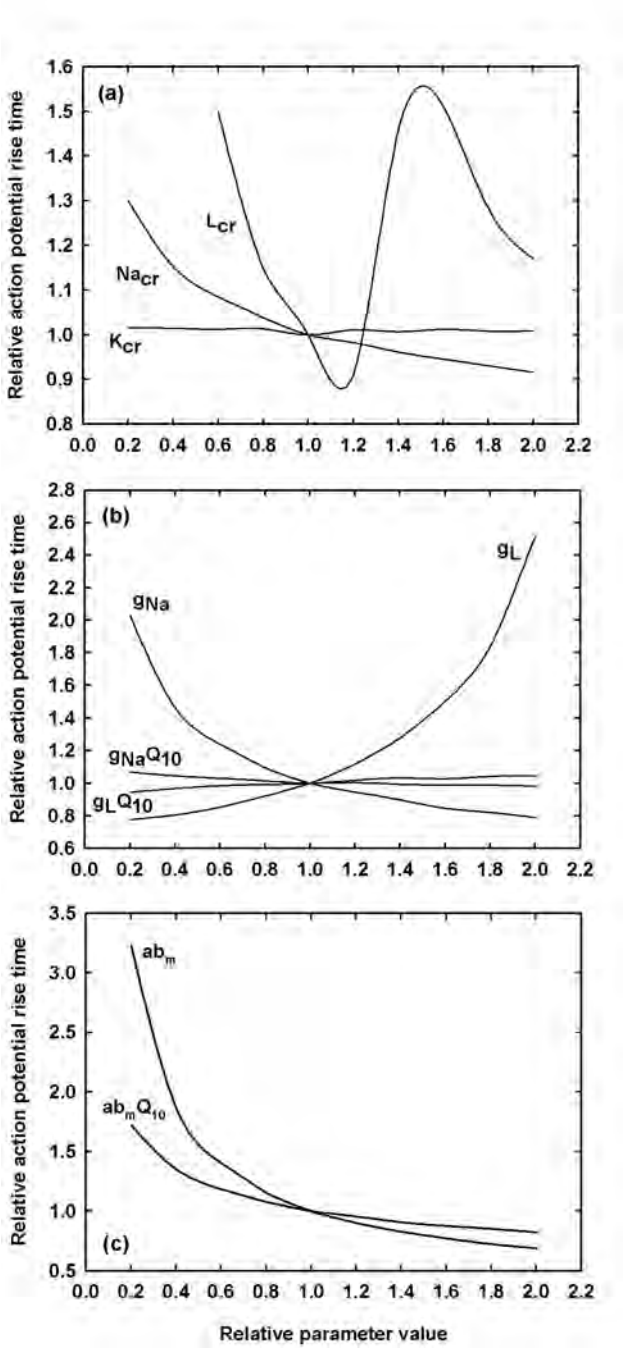

Figure 3.2: Relative sensitivity of action potential rise times to (a) sodium ion (Na_{cr}), potassium ion (K_{cr}) and leakage (L_{cr}) concentration ratios; (b) sodium conductance (g_{Na}), sodium conductance Q_{10} factor ($g_{Na}Q_{10}$), leakage conductance (g_L) and leakage conduction Q_{10} factor (g_LQ_{10}); and (c) Q_{10} factor for sodium activation rate equation (ab_mQ_{10}) and acceleration factor for sodium current activation and deactivation (ab_m). All calculations were performed at 25 °C. Parameter values were varied between 20 and 100% of the values used in the nodal model.

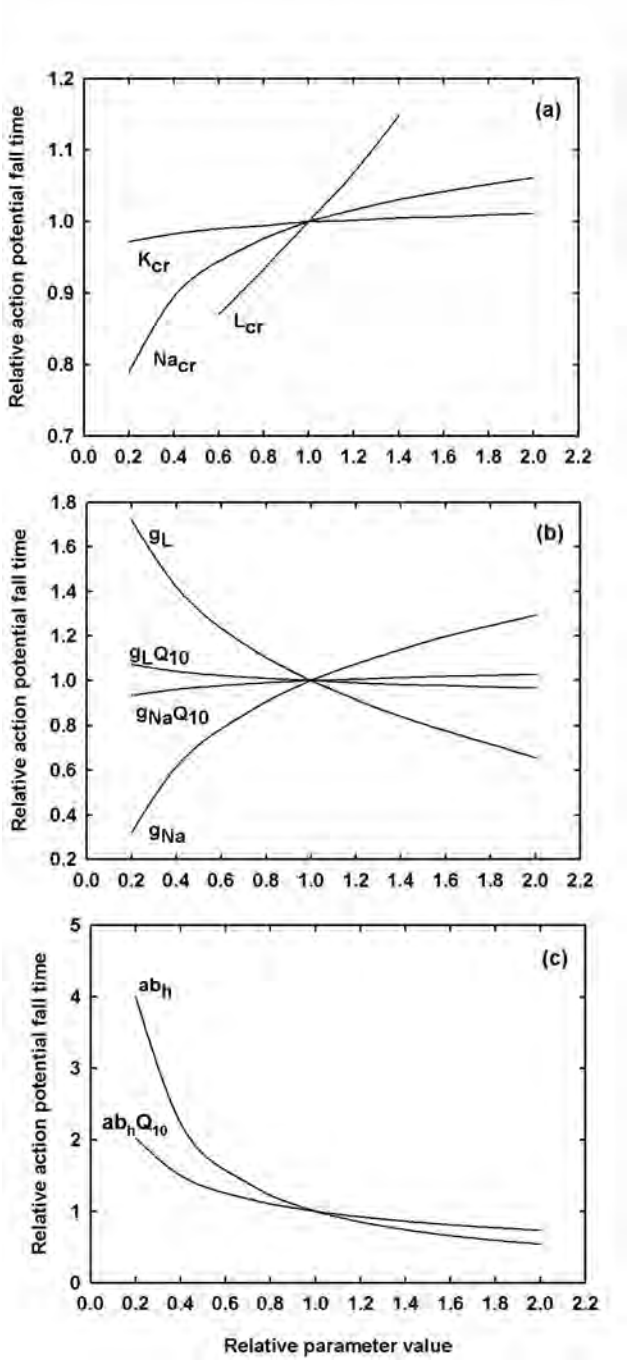

Figure 3.3: Relative sensitivity of action potential fall times (a) sodium ion (Na_{cr}), potassium ion (K_{cr}) and leakage (L_{cr}) concentration ratios; (b) sodium conductance (g_{Na}), sodium conductance Q_{10} factor ($g_{Na}Q_{10}$), leakage conductance (g_L) and leakage conduction Q_{10} factor (g_LQ_{10}); and (c) Q_{10} factor for sodium activation rate equation (ab_hQ_{10}) and acceleration factor for sodium current activation and deactivation (ab_h). All calculations were performed at 25 °C. Parameter values were varied between 20 and 100% of the values used in the nodal model.

increased the rise time by 150%, while decreasing the fall time by 35%. Decreasing g_L by 80% decreased the rise time by 22%, while the fall time increased by 70%. Similar to $g_{Na}Q_{10}$, the leakage conductance Q_{10} factor values (g_LQ_{10}) influenced the rise and fall times by less than 6%, with decreased values having a slightly larger effect than increased values.

The leakage concentration ratio (L_{cr}) seemed to have a large effect on the rise and fall times (Figures 3.2(a) and 3.3(a)). Fall times increased with an increase in L_{cr}, with no clear trend established for the rise time predictions. No action potentials could be elicited below a relative value of 0.60. In Section 3.2 it was mentioned that the membrane potential ($V(t)$) was offset by the membrane resting potential (V_{rest}), with initial value $V(0) = 0$. Decreasing L_{cr} to a relative value of 0.6 increased the offset value needed to reset $V(t)$ to zero by about -13 mV. Increasing L_{cr} two-fold raised the beginning phase of the AP's up-stroke by about 18 mV and the tail part and subsequent recovery phase of the down-stroke by about 21 mV creating the impression that the AP did not inactivate. These changes thus distorted the AP's shape. Considering the triangle method used to calculate the rise and fall times, the shape characteristics might be less sensitive to L_{cr} than indicated.

The rising phase of the AP was influenced by sodium activation kinetics (Figure 3.2(c)), with sodium inactivation kinetics having a less than 5% influence. The opposite held true for the falling phase (Figure 3.3(c)). Potassium activation kinetics had a less than 2% influence on either phase; and potassium ion concentration ratio (K_{cr}) less than 3%. K_{cr} showed the same tendency as L_{cr} to lower or raise the up-stroke and down-stroke current level, but much less pronounced as in L_{cr}.

3.3.2 Action potential amplitude

Calculated amplitudes around 116.7 mV were obtained at 20 and 25 °C, with the amplitude decreasing by less than 1% from 20 to 25 °C, while at 37 °C the amplitude was slightly larger than 115 mV. These results followed the trend of an amplitude decrease with temperature increase (Buchthal and Rosenfalck, 1966; Schwarz and Eikhof, 1987; Frijns *et al.*, 1994; Wesselink *et al.*, 1999).

The amplitude was most sensitive to g_{Na}, g_L and Na_{cr}, while it appeared to be less

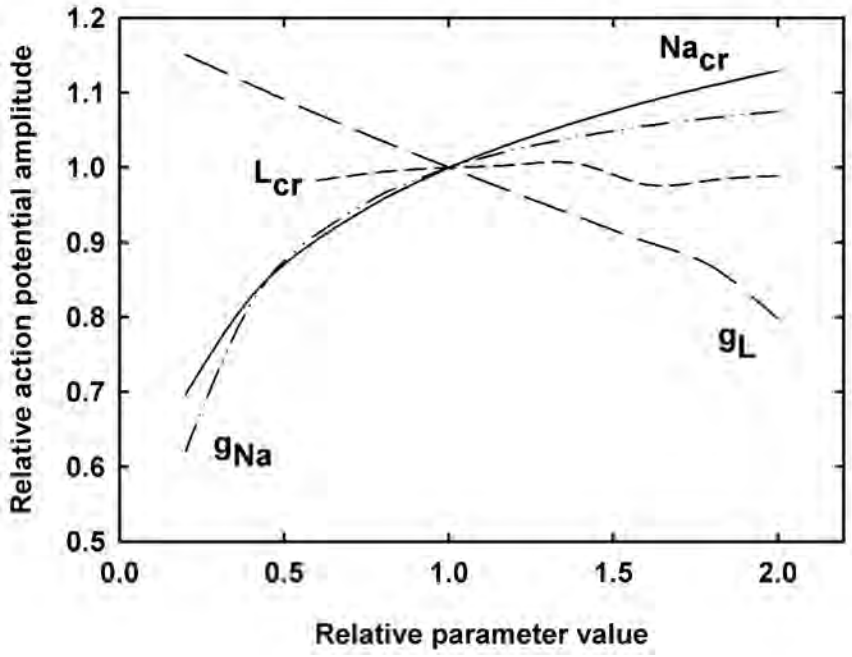

Figure 3.4: Relative sensitivity of action potential amplitude to sodium and leakage conduction and ion concentration ratio parameters, calculated at 25 °C. Nomenclature is the same as in Figures 3.2 and 3.3. Parameter values were varied between 20 and 100% of the values used in the nodal model.

so for L_{cr} (Figure 3.4). However, when the amplitude was corrected for the rise in the tail part of the action potential, in effect the amplitude was increased when L_{cr} was decreased, while an increase in L_{cr} decreased the amplitude. The corrected curve thus closely followed the g_L curve. For the other parameter values the variation in amplitude was less than 2.5%.

3.3.3 Strength-duration relationships

Strength-duration relationships were calculated at temperatures between 20 and 37 °C; with a calculated chronaxie time constant (τ_{ch}) of 65.5 μs at 37 °C (Table 3.3).

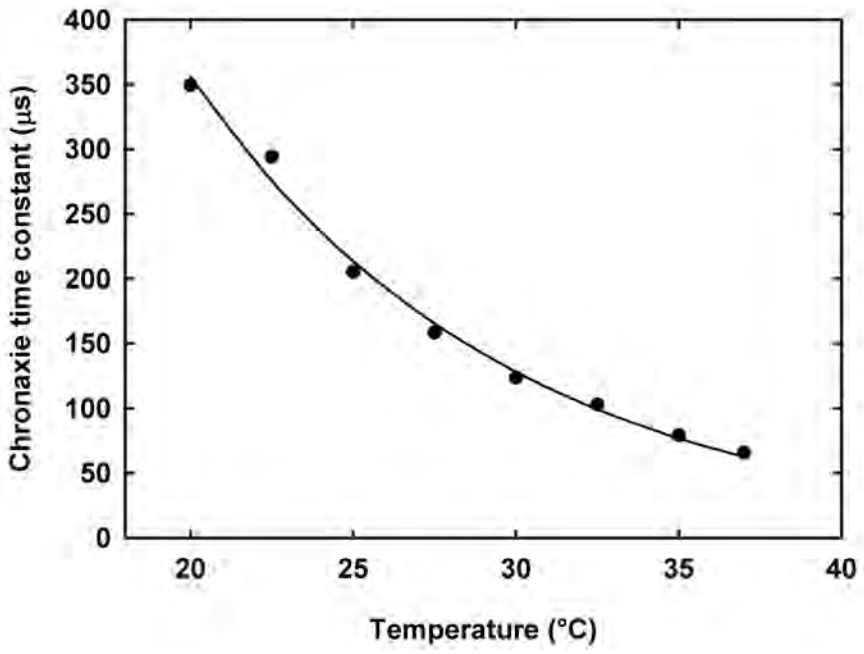

Figure 3.5: Temperature dependence of the chronaxie time constant for a single Ranvier node. Filled symbols indicate the simulated chronaxie times. The curve is obtained by regression fitting of a decaying exponential function, and corresponds to a Q_{10} of $(2.78)^{-1}$.

τ_{ch} values increased by 89% with a temperature decrease from 37 to 30 °C, corresponding to a Q_{10} factor of $(2.48)^{-1}$ (Figure 3.5), while rheobase current values decreased by

51.6% over the same temperature interval. The temperature dependence of τ_{ch} could be fitted by an exponential relationship, corresponding to a Q_{10} factor of $(2.78)^{-1}$, which is larger than the calculated Q_{10} factor.

3.4 DISCUSSION

The development of a model of a Ranvier node in a general human peripheral sensory nerve fibre was based on the HH model, modified with recorded ionic membrane current data from single human myelinated peripheral nerve fibres (Reid *et al.*, 1993; Scholz *et al.*, 1993; Schwarz *et al.*, 1995; Reid *et al.*, 1999). Temperature dependence of all parameters was included. Simulation results suggested the possibility of modifying the original HH model to describe AP excitation characteristics in human sensory nerve fibres.

Rate equation Q_{10} factors, for a reference temperature of 20 °C, tend not to differ much between previously developed models. Q_{10} factors of 2.9 and 3 are used for sodium inactivation and potassium activation respectively (Schwarz and Eikhof, 1987; Schwarz *et al.*, 1995; Wesselink *et al.*, 1999), while 2.2 are most commonly used for sodium activation (Schwarz and Eikhof, 1987; Schwarz *et al.*, 1995). Wesselink *et al.* (1999) used a value of 1.7 for the sodium activation; based on the Q_{10} factor for the measured decrease in rise time between 20 and 25 °C. Moore *et al.* (1978) used a Q_{10} factor of 3 for all rate constants in their standard high-density HH model. Optimisation of these factors for the new nodal model produced a sodium inactivation Q_{10} factor of 1.5, very close to the estimated value of 1.56 describing the experimentally observed decrease in fall time between 20 °C and 25 °C. The potassium activation kinetics had a less than 1% influence on the fall time and thus practically any Q_{10} factor value could be used. However, since this value tends to be fairly similar to the value of sodium inactivation, it was decided to use a value of 1.5 as well. The Q_{10} factor of 2.78 for the sodium activation kinetics was higher than the value of previous models, resulting in a 49% higher sodium activation at 37 °C compared to the Schwarz *et al.* (1995) results. This is in contrast to the 30% lower sodium activation at 37 °C from the Wesselink *et al.* (1999) model. These differences might be attributed to the optimisation procedure. Parameter values were hand-tuned and the possibility exists that the final solution converged to a local optimum in the solution space rather than to the global optimum,

and that a more efficient optimisation routine would be required instead (Huys, Ahrens and Paninski, 2006).

Since I_{Ks} actives and deactivates slowly, and does not inactivate, its influence on the AP shape and amplitude is almost insignificant when nerve fibres are stimulated with short duration pulses (Reid *et al.*, 1993; Schwarz *et al.*, 2006). The relative insensitivity of the simulated characteristics of I_{Ks} compared favourably to the experimental observations. Schwarz *et al.* (1995) measured a leakage current with a leakage equilibrium potential of -84.0 mV at 20 °C, resulting in an L_{cr} of about 0.036. This value is similar to the K_{cr} value (Table 3.2). Since part of the I_{Ks} current is already activated at the resting membrane potential (Schwarz *et al.*, 2006), it might be assumed that a large part of I_L consists of I_{Ks} and not from a current carried by chloride ions as in the original HH model (Hodgkin and Huxley, 1952). Schwarz *et al.* (2006) also showed that increasing the extracellular potassium ion concentration increases the holding current, as well as the amplitudes of the tail currents of recorded I_{Ks} currents. This concentration increase can be simulated by an increase in K_{cr}, and also L_{cr}. An increase in any one of these two parameters led to an increase in the initial AP rising phase up-stroke current, as well as the tail current of the down-stroke and subsequent recovery phase, and was hence in accordance with the Schwarz *et al.* (2006) results.

Scholz *et al.* (1993) measured voltage-dependent sodium single channels at room temperature (about 24 °C) in a Ringer solution with a Na_{cr} of about 14.05. This single channel conductance value can be converted to a value for g_{Na}, provided the Na^+ channel density is known (Hille, 2001). However, no values are known for corresponding human parameters, but for mammals the Na^+ channel densities vary from 700 to 2000 $/\mu m^2$ (Hille, 2001). Using the Scholz *et al.* (1993) values to predict a simulated AP of correct amplitude and shape required a Na^+ channel density of less than 300 $/\mu m^2$. Optimisation of Na_{cr} predicted a lower value than the Scholz *et al.* (1993) value and hence the single channel sodium conductance had to be corrected for the concentration difference. Calculation of g_{Na} then required a Na^+ channel density of 959 $/\mu m^2$. In myelinated nerve fibres a large Na^+ channel density is needed at the Ranvier node to elicit and maintain efficient and rapid propagating APs (Rasband and Trimmer, 2001), and even though the predicted nodal model value fell within the range of mammalian Na^+ channel densities, it might be an underestimation of the real density in human.

It is well known that voltage-dependent sodium channels are more homogeneously distributed along unmyelinated than in myelinated fibres, where the channels mainly cluster in high density at the Ranvier nodes (Salzer, 1997; Vabnick and Shrager, 1998; Boiko, Rasband, Levinson, Caldwell, Mandel, Trimmer and Matthews, 2001). Furthermore, in adult mammalian nerve fibres, one type of sodium channel, $Na_{v1.2}$, is restricted to unmyelinated fibres, whereas a different type, $Na_{v1.6}$, is found at the Ranvier nodes (Boiko *et al.*, 2001). Studies also show that as a myelinated axon matures from an unmyelinated state to a myelinated state, $Na_{v1.2}$ is initially expressed in the unmyelinated fibre and gradually replaced by $Na_{v1.6}$ as the fibre becomes myelinated (Vabnick and Shrager, 1998; Boiko *et al.*, 2001; Rasband and Trimmer, 2001). These two types also activate and inactivate at different voltages (Catterall, Goldin and Waxman, 2005). Differences also exist for voltage-dependent potassium (K_v) channels. For example, unmyelinated fibres have fast delayed rectifying K_v channels, whereas mammalian Ranvier nodes seem to lack these (Hille, 2001) and expresses potassium channels with slower kinetics instead (Taylor *et al.*, 1992; Devaux *et al.*, 2004; Schwarz *et al.*, 2006). Given these differences, it might be necessary to not only modify the model parameters, but also the model equations.

No studies regarding the measurement of strength-duration relationships for single human Ranvier nodes were found in literature. An average chronaxie time constant of 64.9 $\pm$ 8.3 μs is estimated at 37 °C for normal rat Ranvier nodes (Bostock, Sears and Sherratt, 1983). The chronaxie time of 65.5 μs calculated at 37 °C for the human nodal model compared favourably with this estimate. However, when the temperature dependence of the chronaxie time constant is considered, a Q_{10} factor of $(1.39)^{-1}$ is calculated when the temperature is decreased to 30 °C (Bostock *et al.*, 1983). This is almost a factor 2 smaller than the corresponding value for the human nodal model. In the nodal model the single Ranvier node was placed in an infinite, isotropic and homogeneous saline extracellular medium. In *in vitro* measurements the fluidic extracellular medium, in close proximity to the nerve fibre, consists mainly of Ringer or standard extracellular solutions for which the resistivity and corresponding temperature dependence may be different to those of saline. Also, the effect internodes have on the excitability behaviour of nerve fibres was not included in the nodal model. This effect will be studied in Chapter 4 on the temperature dependent excitability behaviour of a cable model representation of a human peripheral sensory nerve fibre.

3.5 CONCLUSION

In this chapter the possibility was examined to modify the HH model to predict excitability behaviour at Ranvier nodes when only the model parameters were modified to those of human, while the equations themselves were left unaltered. From the results it can be inferred that the new nodal model could satisfactorily predict AP shape and amplitude at different temperatures, but chronaxie times were overestimated at temperatures lower than body temperature.

The HH model equations are derived for an unmyelinated nerve fibre. Given the differences that were discussed between the ion channel kinetics and organisation at human Ranvier nodes compared to those in unmyelinated nerve fibres, it might well be that the activation and inactivation rate equations, in their original form, do not adequately describe the kinetics for the ion channel types found at the Ranvier node in a myelinated nerve fibre. Thus, in addition to the modifications made to the model parameters, the equations themselves might need to be modified to explain excitability behaviour in human peripheral sensory nerve fibres more accurately.

However, such an inference might only be drawn after the new nodal model has been incorporated into a more comprehensive nerve fibre cable model and validated against experimentally measured nerve fibre data. In the next chapter this nodal model will be incorporated into a cable model to investigate such excitability behaviour characteristics as refractory time periods and conduction velocity, as well as to better compare simulated and experimentally measured chronaxie times.